Thermodynamics of absorbing solids during short-pulse laser ablation

Patrick Lorazo[a,b], Danny Perez[b], Laurent J. Lewis[b], and Michel Meunier[a]

[a]Département de Génie Physique et Regroupement Québécois sur les Matériaux de Pointe (RQMP), École Polytechnique de Montréal, C.P. 6079, Succursale Centre-Ville, Montréal, Québec, Canada H3C 3A7

[b]Département de Physique et Regroupement Québécois sur les Matériaux de Pointe (RQMP), Université de Montréal, C.P. 6128, Succursale Centre-Ville, Montréal, Québec, Canada H3C 3J7

ABSTRACT

The fundamental mechanisms of matter removal involved in the interaction of short laser pulses with absorbing solids have been investigated using molecular-dynamics/Monte Carlo simulations. This is accomplished under the two following assumptions: (i) the elementary thermodynamic properties of targets (metals and semiconductors) are adequately described by empirical potentials; (ii) in the regime where ablation is thermal, the complete time evolution of the system can be followed in ρ-T-P space and the result mapped onto the equilibrium phase diagram of the material. We find remarkable similarities in the physical pathways to ablation in metals and semiconductors for pulse durations ranging from 200 fs to 400 ps: (i) under conditions of isochoric heating and rapid adiabatic cooling with femtosecond pulses, several mechanisms can simultaneously account for matter removal in the target: spallation, phase explosion, vaporization, and fragmentation; the latter is identified for the first time in the context of laser ablation. (ii) Under nonadiabatic cooling with picosecond pulses, ablation is driven by a "trivial" fragmentation process in the metallic, supercritical fluid; this suggests a pulse duration upper limit for phase explosion of $\sim 10^{-11}$ s.

Keywords: Short laser pulses, ablation mechanisms, metals, semiconductors, molecular dynamics, Monte Carlo

1. INTRODUCTION

The ejection of matter obtained by focusing a short ($\sim 10^{-13}$ to 10^{-8} s) laser pulse onto a surface, i.e., laser ablation, can be regarded as the final stage of a long chain of processes covering several length and time scales. The details depend essentially on the material properties and laser parameters. As an example, the interaction of an ultrashort ($\lesssim 1$ ps) pulse with a metallic surface involves the coupling of the photons with the quasi-free electrons, internal thermalization of the hot electron gas within a few tens of fs, transfer of the excess energy to the ions in a few ps, generation of acoustic waves, melting, rapid expansion, and dilution of the material over several tens of ns.[1] A direct solid-to-plasma transition has also been reported in semiconductors and dielectrics with subpicosecond pulses at irradiances greater than $I_{\mathrm{p}} \sim 10^{13}$ W/cm^2.[2,3]

The complex phenomenology and great diversity of conditions involved in laser ablation suggest a plethora of physical pathways. This poses in turn a serious challenge to the understanding of the underlying fundamental mechanisms: spallation,[4,5] homogeneous nucleation of gas bubbles and phase explosion (or explosive boiling),[3,4,6–9] spinodal decomposition,[10] fragmentation,[5,8,9,11] and vaporization[12] are among the thermal mechanisms that have been proposed. In principle, these can be assessed by identifying the sequence of thermodynamic states through which the system evolves as a result of laser irradiation. In the specific case of absorbing solids under ultrashort pulses, near-threshold time-resolved pump-probe experiments have suggested a universal path by which metals and semiconductors dilute in vacuum.[3] In particular the observation of interference fringes (Newton rings) on a nanosecond time scale has unveiled an optically transparent material trapped between two

Contact author: L.J.L.; E-mail: Laurent.Lewis@UMontreal.CA, Phone: +01-514-343-7721, Fax: +01-514-343-2071

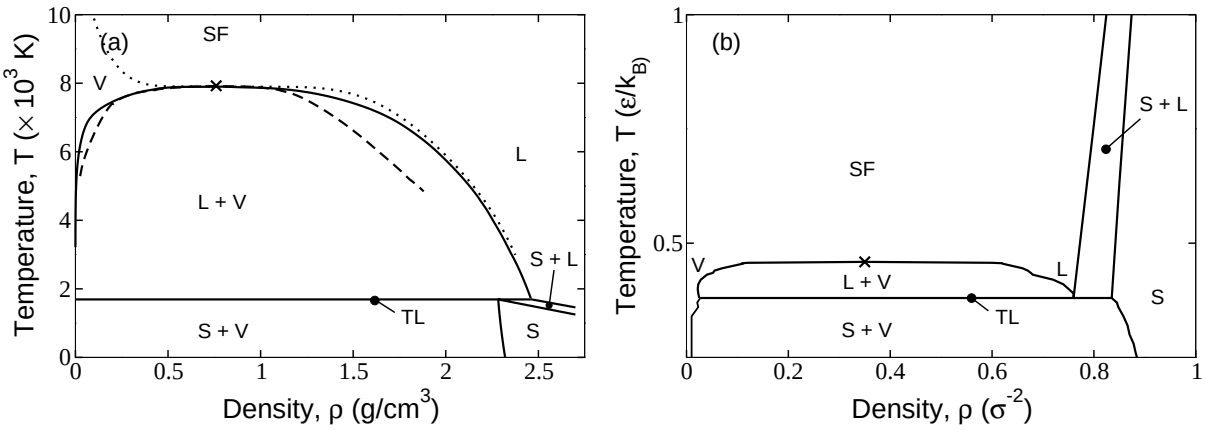

Figure 1. $\rho - T$ projection of the phase diagram of (a) silicon (as obtained from the SW potential) and (b) the two-dimensional LJ potential (truncated and shifted) for which the results are quoted in standard reduced units, i.e., $\epsilon/k_{\rm B}$ for temperature, $\tau = (m\sigma^2/\epsilon)^{1/2}$ for time (m is the atomic mass), and σ^{-2} for density; ϵ and σ are the usual energy and length scales. Cross: critical point (for Si, $\rho_{\rm c} = 0.760$ g/cm^3, $T_{\rm c} = 7925$ K, and $P_{\rm c} = 185$ MPa[14]); dashed and dotted lines: spinodal and critical isobar of Si. The letters S, L, and V refer to the solid, liquid, and vapor phases, respectively; SF: supercritical fluid (for $T > T_{\rm c}$ and $P > P_{\rm c}$); TL: triple line. See text for additional details.

sharp interfaces, which has been interpreted as a phase transition within the liquid-vapor regime enclosed by the binodal, i.e., phase explosion. In general, however, an assessment of the thermodynamic pathways to ablation by experimental means remains a difficult task.

In this paper we present an overview of the work we have conducted on laser ablation using a combined molecular-dynamics (MD)/Monte Carlo (MC) scheme.[5,8,9,13] We investigate the thermal regime, where equilibrium between the electrons and the ions has been achieved by the time matter removal occurs, i.e., for $I < I_{\rm p}$. This is accomplished for two model systems representing two classes of materials, namely metals and covalent semiconductors. We follow the complete thermodynamic evolution of the systems in ρ-T-P space for pulse durations of 200 fs to 400 ps and show that, in spite of different routes from solid to liquid, the physical pathways to ablation are remarkably analogous.

2. COMPUTATIONAL METHODS

2.1. Models

In order to draw a general portrait of the matter removal dynamics in absorbing solids, we have focused on two important classes of materials: covalent semiconductors and metals. This translates into two different but complementary models.

2.1.1. Covalent semiconductors

The first model, of which a summary is given in Ref. 9, is meant to give a precise description of laser-matter interaction. We have chosen to simulate silicon, but the following picture also applies to other group IV and III-V semiconductors. Full details will be given elsewhere.[15] In brief, the laser pulse with $\lambda_{\rm L} = 266$ nm and duration $\tau_{\rm L}$ (FWHM) provides photons which generate hot "carriers" via interband or intraband (inverse bremsstrahlung) transitions over a penetration depth $\delta \approx 5 - 10$ nm (in both c-Si and l-Si). The electrons and holes subsequently relax through a cascade of scattering events, each with its own characteristic collision time. Here, a carrier is a "fictitious" particle obeying Drude dynamics within a standard MC scheme: it diffuses ballistically between two successive collisions which instantaneously change its velocity and energy, but not its position. In the tetravalent semiconducting crystal, the collision processes include Auger recombination, impact ionization, carrier-carrier ($\tau_{\text{c-c}} \sim 10$ fs), and carrier-phonon scattering ($\tau_{\text{c-ph}} \sim 10$ fs). The latter process is responsible for the energy transfer from the electrons to the ions with temperatures $T_{\rm e}$ and T, respectively: it is achieved by giving a

quantum of energy (a few tens of meV) to the closest atom if $T_e > T$. If a sufficient amount of energy is deposited into the system, melting to a *metallic*, sixfold-coordinated, liquid phase (with electron density $\sim 10^{23}$ cm^{-3}) occurs. This is locally simulated by promoting the remaining valence electrons (up to four per atom) to the conduction band. In the liquid, electrons undergo carrier-carrier and carrier-phonon scattering events.

The atoms are followed in phase space using classical MD and interact via the Stillinger-Weber (SW) potential;[16] the latter provides a satisfactory description of both solid and liquid phases of silicon.[17] Figure 1a displays the phase diagram of silicon. The spinodal and binodal lines (which meet at the critical point) have been obtained from Refs. 14 and 18, respectively. The triple line at the melting temperature $T_m = 1691$ K (close to the experimental value of 1683 K) and the solid-vapor coexistence curve have been taken from Ref. 19. In addition, the solid-liquid region and the critical isobar were determined from NVT simulations. Finally, note that: (i) it is possible for a system to access the metastable region (between the binodal and spinodal) in a homogeneous state; however, for sufficiently long waiting times, widespread and simultaneous nucleation of gas bubbles in the liquid, i.e., explosive boiling, is expected to occur.[3] (ii) In the region below the spinodal, a homogeneous system is mechanically unstable against small perturbations; here, the liquid-to-gas transition is described, rather, by a spinodal decomposition process.[10] (iii) Silicon *densifies* upon melting (provided heating is carrier out in a time longer than the characteristic time scale for mechanical response of the material); this is analogous to the case of other covalent semiconductors but contrary to that of metals (see Fig. 1b and text below).

2.1.2. Metals

In contrast, the second model is "generic" and is not meant to reproduce light-matter interactions in a rigorous manner; rather, it is expected to possess the essential features which are relevant to a "general" description of laser ablation (see Refs. 5 and 8 for complete details). It combines a two-dimensional Lennard-Jones (LJ) model for MD with a simplified MC scheme for carriers. This approach allows larger systems and longer pulse durations to be investigated. Figure 1b shows the corresponding phase diagram for which two remarks are in order: (i) in spite of the lower dimensionality of the system, the phase diagram is qualitatively similar to that of a metal; hence, it is expected to capture the fundamental pathways to ablation in metallic systems. (ii) As noted above, the route to melting differs in covalent semiconductors and metals. However, the liquid-vapor and supercritical regions exhibit features that are common to the two classes of materials. Moreover, both systems are metallic in the liquid state. We show below that these similarities suggest a universal behavior for ablation in absorbing solids over a large range of pulse durations.

2.2. Thermodynamic Analysis

In the regime where ablation is thermal, it is reasonable to assume that most of the evolution of the system occurs under conditions of local equilibrium between the electrons and the ions. Thus, in this context, short-pulse laser irradiation can locally be described as a sequence of thermodynamic states in the equilibrium phase diagram of the material. This has been accomplished for the two model systems described above using a method we have recently developed and described at length elsewhere.[5,8] In short, the density, temperature, and pressure for various sections of the target are obtained at regular intervals and the result mapped onto the corresponding phase diagram. Three branches are computed: macroscopic (or average), dense (for clustered atoms in the solid and/or liquid), and gas. The location in the phase diagram where the average and dense branches split indicates the appearance of voids and therefore identifies the mechanism by which matter removal occurs. As shown in Sect. 3, this method constitutes a simple, yet powerful tool to gain insight into the transient states induced in a material by laser irradiation.

3. PHYSICAL PATHWAYS TO ABLATION

We first examine the thermodynamic trajectories of absorbing solids under ultrashort pulses (Sect. 3.1). The conclusions are twofold: (i) close to the threshold energy for ablation, our results confirm that an inhomogeneous mixture of liquid and gas expands between two optically flat interfaces following homogeneous bubble nucleation in a superheated liquid, in agreement with Sokolowski-Tinten *et al.*;[3] far from the threshold, a new mechanism in the context of laser ablation, i.e., (non-trivial) fragmentation, accounts for the breakup of the rapidly expanding supercritical fluid. (ii) In general, several mechanisms can occur simultaneously in different parts of the target.

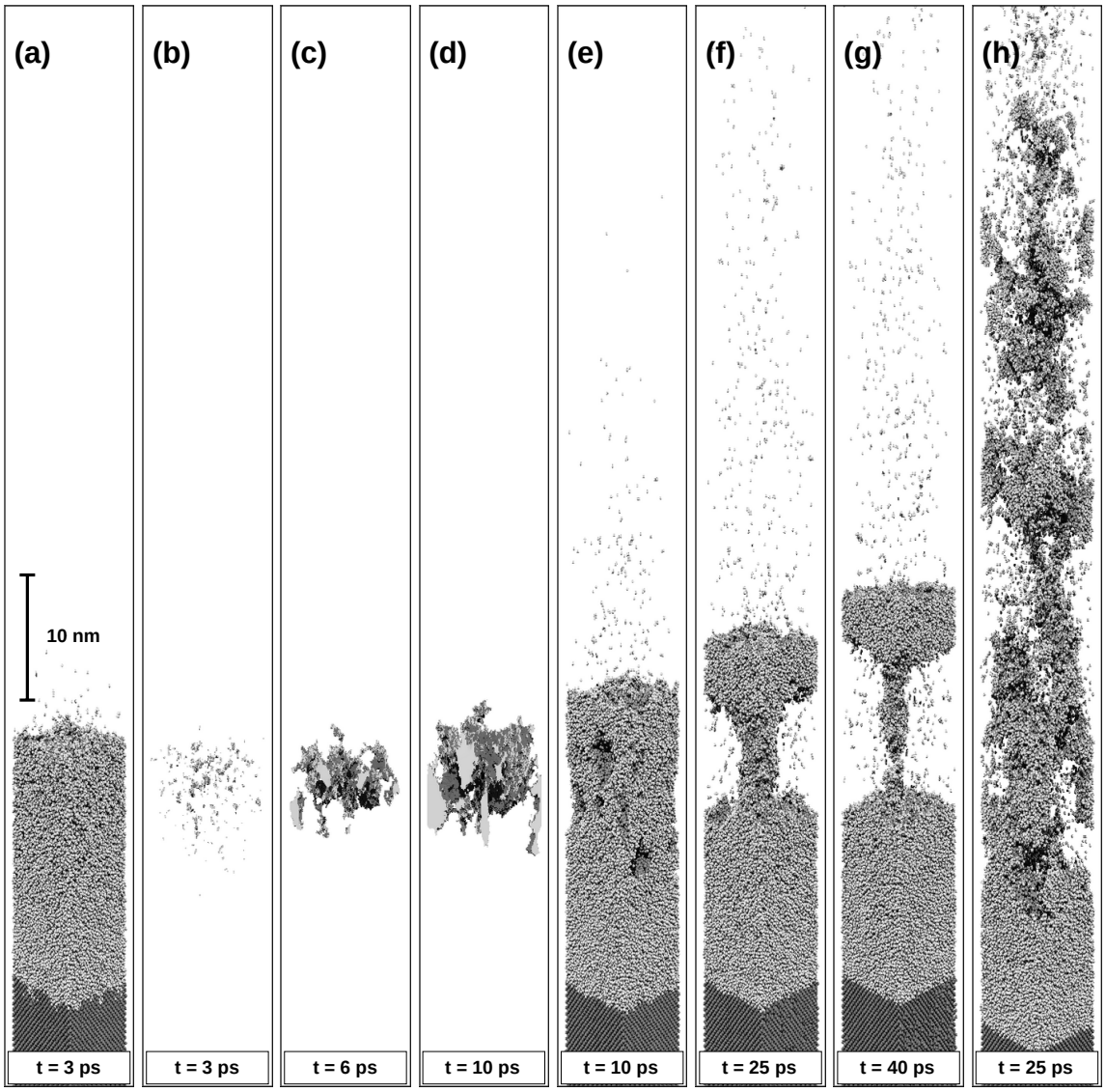

Figure 2. Snapshots illustrating the morphological changes induced in a Si(100) substrate by a 266 nm, 500 fs pulse for two fluences: (a)-(g) 0.225 J/cm^2, with a view of the growing cavity within the expanding liquid layer in (b) to (d); (h) 0.375 J/cm^2. Each pulse begins at $t = 0$. In (a) and (e) to (h): dark gray: crystalline silicon; light gray: (metallic) liquid silicon.

In the case of picosecond pulses (Sect. 3.2), we find that phase explosion is suppressed by a combination of slower expansion and efficient thermal conduction. As a result, matter removal is driven by a "trivial" fragmentation process associated with the regions undergoing supercritical expansion.

3.1. Femtosecond Pulses

Figures 2a-2g illustrate the structural and phase changes induced in a Si(100) substrate by a 500 fs pulse *at* the threshold energy for ablation, $F_{\rm th}^{\rm a} = 0.225$ J/cm^2. The irradiance is 5×10^{11} W/cm^2, well below $I_{\rm p}$. The simulation is for a slab originally consisting of 142560 atoms ($10 \times 10 \times 30$ nm^3) and equilibrated at 300 K. The result of laser irradiation can be described as follows: (i) shortly after the end of the pulse ($t \approx 1$ ps), a 15-nm-thick, hot, highly-pressurized liquid layer has developed at the surface (not shown); this is too short time

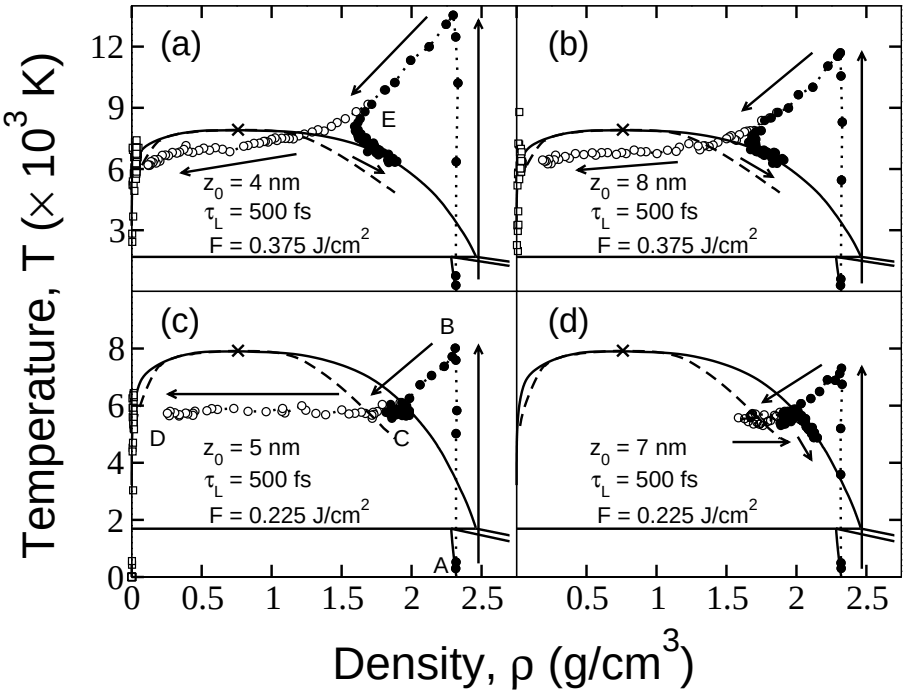

Figure 3. Time evolution of the system in the $\rho - T$ plane for the two cases illustrated in Fig. 2. The thermodynamic trajectories are for different fluences and depths z_0 below the original surface (as indicated). Open circles and dotted line: macroscopic branch; full circles: dense branch; squares: gas branch. Arrows indicate the flow of time. Capital letters refer to locations in the phase diagram, of which a description can be found in Fig. 1a.

for significant expansion to occur. (ii) In order to release the pressure and mechanically equilibrate with the ambient vacuum, the molten layer starts to expand; acoustic waves are also emitted downward into the cold, crystalline bulk. Figure 2a displays a snapshot of the system about 3 ps following the onset of the pulse: the expanding liquid layer is still homogeneous at this point, as can be appreciated from the corresponding view of the voids in Fig. 2b; as shown below, this precisely corresponds to the moment at which the system enters the metastable region and becomes superheated. (iii) The further expansion of the material is associated with the rapid growth of a cavity below the surface: the latter, with a volume of 50 nm^3 at $t = 6$ ps, has grown to more than 200 nm^3 by $t = 10$ ps (Figs. 2c and 2d). It eventually percolates through the slab, leading to the ejection of a liquid layer with a velocity of ≈ 300 m/s (Figs. 2e-2g). It should be noted that the above cavity does not correspond to what one would expect from classical nucleation theory, i.e., a spherical bubble; rather, it resembles a web-like structure, in agreement with simulations of a superheated LJ liquid.[20]

Figs. 2a-2g illustrate the nucleation of a gas in a liquid between two well-defined interfaces near the threshold energy: the ablation front (or surface) and the boundary separating the ablated and nonablated regions; this is consistent with the picture reported in Ref. 3, hereby suggesting an ablation process mediated by phase explosion. This is confirmed in Fig. 3c showing a typical thermodynamic trajectory for a section of the ablated region and initially located 5 nm below the surface. The starting point is a solid at $\rho_0 = 2.33$ g/cm^3 and $T = 300$ K (marked A). The subsequent scenario is as follows: (i) the incoming photons are rapidly converted into thermal energy (i.e., phonons), roughly on a time scale of a ps. As a result (and as noted above), heating occurs essentially at constant volume ($\rho \approx \rho_0$) to a state at high temperature (≈ 8000 K) and pressure (≈ 12 GPa) (B). Two remarks are in order at this point: (a) the system crosses the triple line during the heating process, hereby melting in the liquid region or possibly even in the liquid-vapor regime. A transition to a liquid state at *solid* density and relatively low temperatures ($T \approx T_{\rm m} \ll T_{\rm c}$) is thus possible in covalent semiconductors because the initial state of the system lies below the triple line. This contrasts with the case of metals which can be heated significantly above $T_{\rm c}$ without melting (see below). (b) The strong electronic excitations achieved in covalent semiconductors

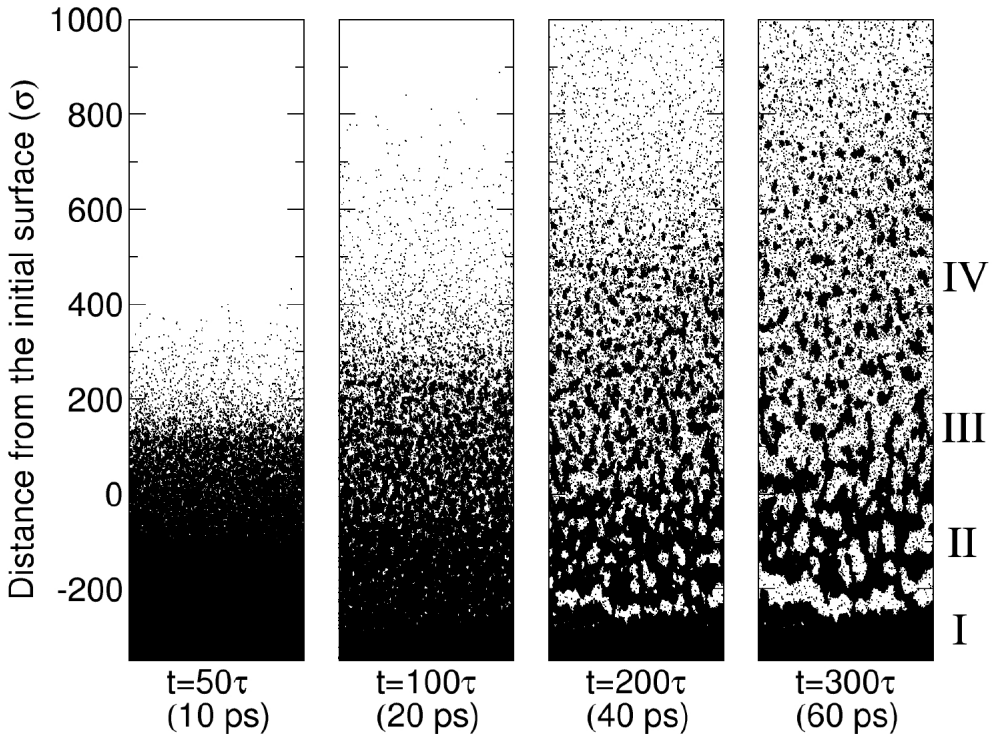

Figure 4. Snapshots of a simulation for the two-dimensional LJ model. The pulse duration (FWHM), absorption coefficient, and fluence are $\tau_{\rm L} = \tau$ ($\approx$ 200 fs), $\alpha = 0.006\sigma^{-1}$ [$\approx$ (36 nm)$^{-1}$], and $F = 900\epsilon/\sigma$, respectively. Roman numerals identify different locations in the remaining target (I) and expanding plume (II, III, and IV). The simulation is for a slab initially equilibrated at a low temperature and composed of 200000 atoms forming a triangular lattice with 500 and 400 atomic layers in the x and y (parallel to the incident pulse) directions, respectively.

with subpicosecond pulses can cause a rapid collapse of the diamond structure, i.e., non-thermal melting of the crystal;[21] this phenomenon cannot be described by empirical potentials such as SW. However, it is reasonable to assume that the details of the solid-to-liquid pathway will not influence the *nature* of the ablation process occurring on much longer time scales. (iii) The pressure is then released by mechanical expansion: the material cools by converting thermal energy into potential and translational energies, thus approaching the liquid-gas region. The rapid expansion is said to be adiabatic and, consequently, isentropic: the system passes from point B to the superheated state C in a time of about 2 ps, i.e., too short for any significant thermal conduction to occur. Figures 2a and 2b illustrate the system shortly after it has reached the metastable region (C): as noted above, the expanding molten layer is still homogeneous. (iv) The final stage involves the nucleation of a gas in the superheated liquid, as indicated by the split of the dense and macroscopic branches and depicted in Figs. 2c-2g. Together with the concomitant appearance of a gas branch, this reveals a decomposition of the metastable phase into a mixture of liquid and gas (C→D), i.e., an explosive boiling process. The same conclusions can be drawn from an inspection of the trajectories in the $\rho - P$ and $P - T$ projections of the phase diagram.

Figures 3a and 3b suggest a different picture for the dynamics of matter removal; this is portrayed in Fig. 2h for a fluence of $1.7F_{\rm th}^{\rm a}$. Two observations readily emerge from a comparison with near-threshold ablation: (i) the plume is not characterized by a well-defined ablation front, i.e., matter removal does not involve the expulsion of a nm-thick liquid shell but, rather, the ejection of clusters; (ii) the plume expands noticeably faster, as can be appreciated from Figs. 2f and 2h, which picture the system at equal times for both fluences. These observations can be understood by looking at a typical thermodynamic trajectory for a section of the target

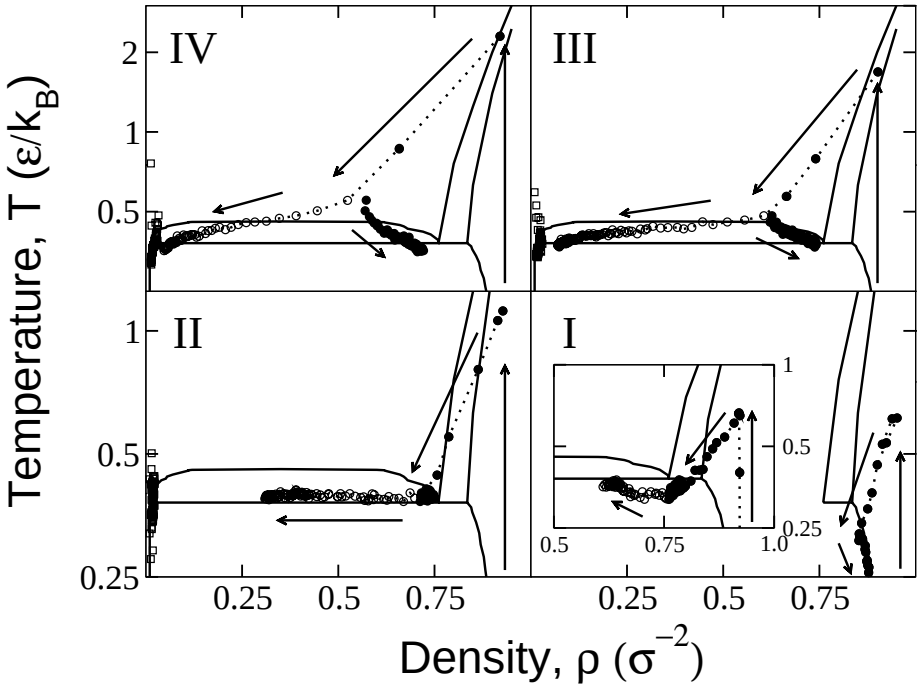

Figure 5. Time evolution of the system in the $\rho - T$ plane for the four different locations (I-IV) identified in Fig. 4. Inset to I: thermodynamic trajectory from a different simulation showing spallation in the solid-vapor coexistence region ($\tau_{\rm L} = \tau$, $\alpha = 0.01\sigma^{-1}$, and $F = 150\epsilon/\sigma$). See Figs. 1b and 3 for a description of the phase diagram and for the definition of symbols and lines, respectively. Note the logarithmic scale for the temperature axis.

undergoing ablation, as illustrated in Fig. 3a for a region initially located a few nm below the surface. As with near-threshold ablation, irradiation by an ultrashort pulse causes the system to be heated at constant volume to a final, high temperature (≈ 13000 K) and pressure (≈ 23 GPa), supercritical state. A rapid isentropic expansion in vacuum follows during which the system approaches the liquid-vapor regime as it adiabatically cools. However, the latter is not reached in a homogeneous state: the split between the dense and macroscopic branches occurs in the supercritical fluid region, i.e., *outside* of any phase coexistence region (marked E). Clearly, matter removal is not, in the present case, the result of a phase transition and cannot be attributed to phase explosion nor spinodal decomposition.

The breakup of an expanding supercritical fluid during short-pulse laser ablation has recently been reported by Perez and Lewis for the two-dimensional LJ model described in Sect. 2.1.2.[5,8] Under ultrashort-pulse (fs) laser irradiation, the rapid expansion of the material can be such that the equilibrium structure can no longer be preserved by atomic diffusion. If this is so, the expanding fluid dissociates into clusters, a phenomenon called (non-trivial) fragmentation; in this context, the average size of the fragments depends on the local strain rate, i.e., the translational velocity *gradient* normal to the surface.[22]

A typical simulation for a pulse duration equal to τ (≈ 200 fs) is presented in Fig. 4; the optical penetration depth is $\delta = 36$ nm, i.e., comparable to that of metallic systems (~ 10 nm). The corresponding thermodynamic trajectories are illustrated in Fig. 5; as mentioned previously, the LJ phase diagram is expected to capture the elementary physical pathways to ablation in metals. Here, three distinct regions need to be distinguished; each corresponds to a different initial depth below the surface and, therefore, a different injected energy: the nonablated region (I) and, within the plume, the slowly (bubble-like, II) and rapidly (cluster-like, IV) expanding regions separated by a boundary (III); a fourth region where the plume is essentially composed of individual atoms is also present (out of range in Fig. 4). Remarkable similarities can be drawn with matter removal in silicon: (i) at near-threshold energies ($F = F_{\rm th}^a$ for Si; region II near the boundary with the nonablated material

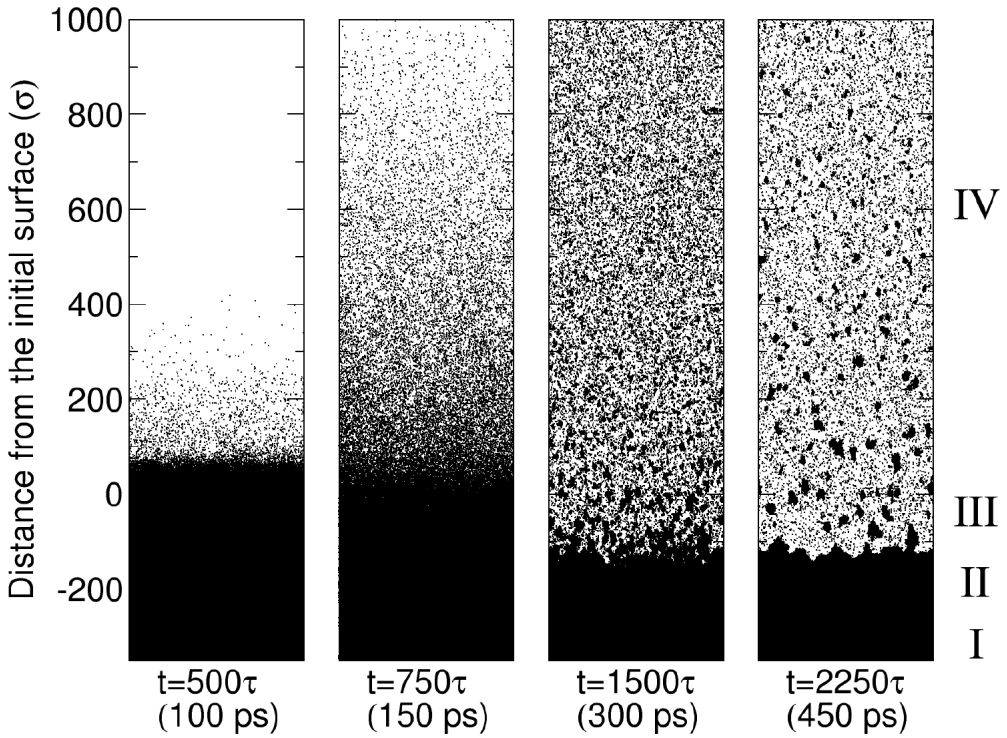

Figure 6. Snapshots of a simulation for the two-dimensional LJ model. The pulse duration (FWHM), absorption coefficient, and fluence are $\tau_{\rm L} = 500\tau$ (≈ 100 ps), $\alpha = 0.006\sigma^{-1}$ [$\approx (36\ {\rm nm})^{-1}$], and $F = 900\epsilon/\sigma$, respectively. Roman numerals identify different locations in the remaining target (I and II) and expanding plume (III and IV). The simulation is for a slab initially composed of 200000 atoms forming a triangular lattice with 500 and 400 atomic layers in the x and y directions, respectively.

for the LJ model), ablation is brought about as the system adiabatically cools into the metastable region where widespread, i.e., homogeneous nucleation of gas bubbles in the superheated liquid sets in. (ii) At higher injected energies ($F = 1.7F_{\rm th}^{\rm a}$ for Si; region IV for the LJ model), the fluid fragments into clusters during its rapid, supercritical, expansion toward the two-phase regime. (iii) In both systems, a complete vaporization of the ejected material into individual atoms is also observed at very high energies.[5]

The above differences in expansion dynamics for a system undergoing an isentropic expansion in vacuum can be interpreted within a one-dimensional self-similar rarefaction wave model.[3,5] Here, the increase in flow (translational) velocity, du, for an infinitesimal increase in density, dρ, is proportional to the speed of sound, c(ρ). In the case of a material initially heated at constant density ρ_0, the translational velocity at density ρ_f reads as

$$u_f(\rho_f, S) = \int_{\rho_0}^{\rho_f} \left(\frac{c(\rho)}{\rho}\right)_S d\rho, \tag{1}$$

where S is the entropy. As stated in Ref. 3, the entrance into the liquid-vapor region is characterized by a sharp drop in $c(\rho)$ and, consequently, a value of u_f essentially *independent* on ρ_f and S.[5] This is not expected for a supercritical expansion during which the material does not experience a drastic decrease of the velocity of sound, thus leading to higher flow velocities that are strongly dependent upon density and entropy. The consequences are twofold: (i) at near-threshold energies, cooling of the system occurs into the metastable region; hence, the different sections of the material (following different subcritical isentropes) possess similar translational velocities.

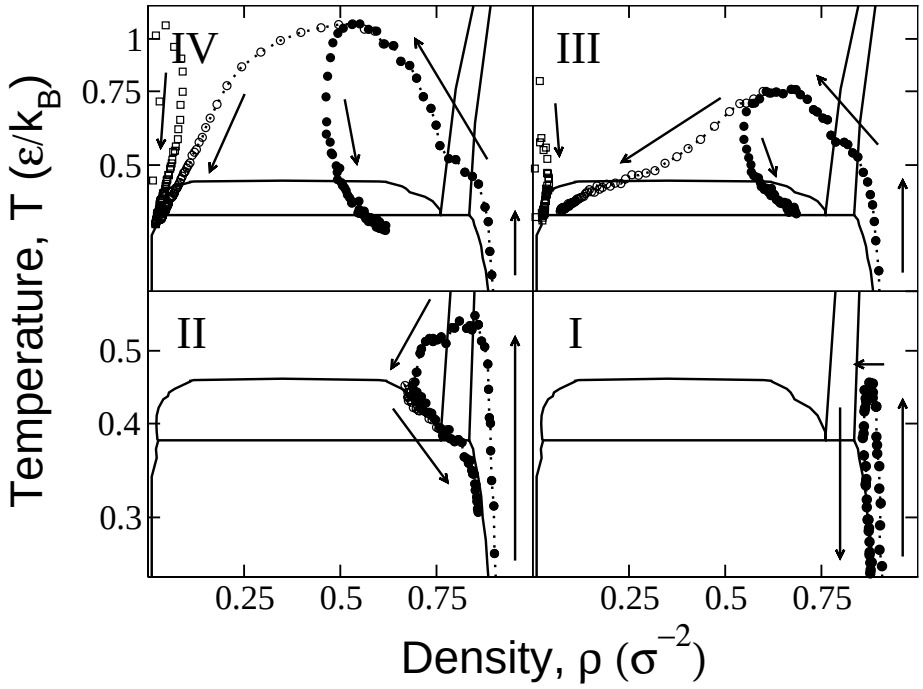

Figure 7. Time evolution of the system in the $\rho - T$ plane for the four different locations (I-IV) identified in Fig. 6. See Figs. 1b and 3 for a description of the phase diagram and for the definition of symbols and lines, respectively. Note the logarithmic scale for the temperature axis.

As a result, the flow velocity gradient varies slowly across the molten layer thus characterized by step-like density profile. (ii) At higher energies where the system expands supercritically, a steeper flow velocity gradient and, therefore, a significantly higher expansion rate, $\dot{\rho}$, are anticipated. This has the following implications: (a) the density is expected to drop smoothly across the molten layer; i.e., no steep ablation front should be visible. (b) If $\dot{\rho}$ is high enough, a (non-trivial) fragmentation process follows; for systems undergoing a slower expansion, "trivial" fragmentation is also possible (see Sect. 3.2). In any case, the expanding material is characterized by a smoother ablation front.[5] This is confirmed in Figs. 2h and 5 (region IV) and supported by time-resolved pump-probe experiments where Newton rings are observed to disappear above a characteristic threshold fluence.[23, 24]

Hence, the above results suggest common physical pathways to ablation in metals and semiconductors under ultrashort pulses. Nevertheless, the following comments are in order: (i) contrary to covalent semiconductors, the initial state of a metal does not lie below the triple line. Thus, the rapidly-heated system can remain *solid* at temperatures in excess of T_c (see Fig. 5): here, melting does not occur during heating but, rather, as the material cools and crosses the solid-liquid region during its subsequent expansion. (ii) In metals, near-threshold ablation can result from spallation whereby solid material is ejected as the system becomes mechanically unstable in the solid-vapor region (inset in Fig. 5; see Ref. 5 for details); at lower energies associated with sections of the nonablated material, the system is, rather, cooled by thermal diffusion along the *solid*-vapor coexistence curve (region I in Fig. 5). This differs in Si where the lowest energy at which matter removal is observed involves explosive boiling and, therefore, the expulsion of a liquid: in covalent semiconductors, ejection of *solid* material under fs pulses seems very unlikely since melting is unavoidable during the heating process. In this context, the threshold is presumably governed by a competition between, on one hand, expansion and bubble nucleation, which favor phase separation, and, on the other hand, thermal conduction which tends to cool the liquid along the *liquid*-vapor coexistence curve (Fig. 3a).

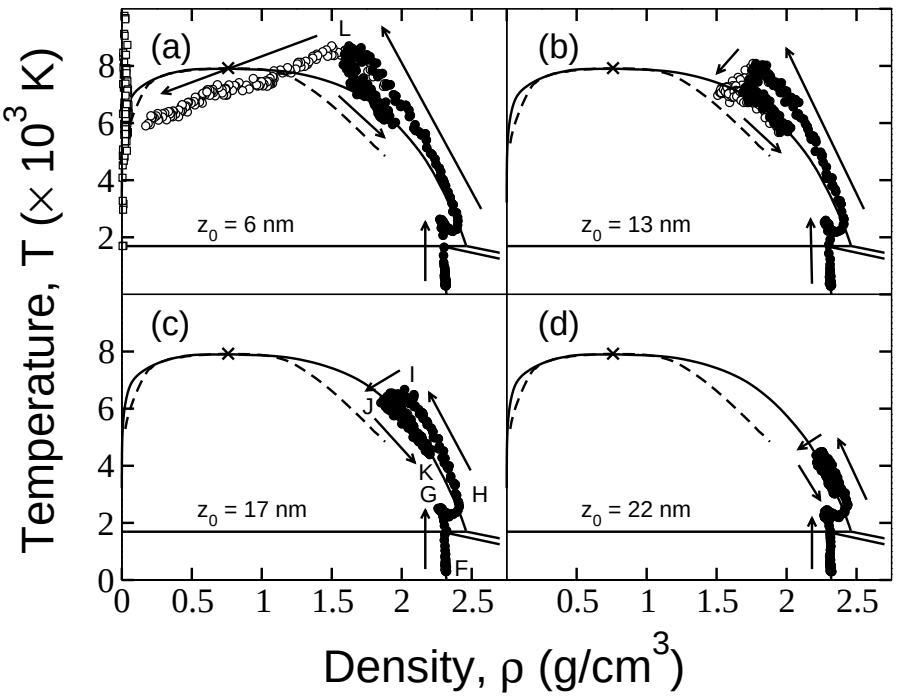

Figure 8. Time evolution in the $\rho - T$ plane for a 266 nm, 25 ps pulse at 0.35 J/cm^2 incident onto a Si(100) substrate. The thermodynamic trajectories are for different depths z_0 below the original surface (as indicated). See Fig. 3 for the definition of symbols and lines. Capital letters refer to locations in the phase diagram, of which a description can be found in Fig. 1a.

3.2. Picosecond Pulses

In Sect 3.1, we have shown the relevance of phase explosion in near-threshold femtosecond ablation of metals and semiconductors, thus confirming the scenario proposed in Ref. 3. At higher injected energies, our simulations have enlightened the role of a new mechanism in the context of laser ablation: (non-trivial) fragmentation. In the following, we give strong evidence for a matter removal process governed by "trivial" fragmentation in absorbing solids for pulse durations in excess of a few tens of ps.

The result of a simulation for the LJ system under ps irradiation is displayed in Fig. 6. The pulse duration has increased by a factor of 500; however, the fluence and optical penetration depth have remained *unchanged*. A visual inspection reveals a picture that is significantly different than that of Fig. 4. In particular, the plume does not show regions characterized by a bubble-like structure or a steep ablation front but, rather, exhibits the presence of small clusters (regions III and IV); larger fragments are also observed at lower fluences. This suggests a mechanism other than explosive boiling.

Figure 7 confirms a qualitatively different reaction of the target to laser irradiation: heating is slower and, in contrast to fs irradiation, substantial expansion occurs during the pulse (II, III, and IV); as a result, the system melts, i.e., crosses the solid-liquid coexistence region, as it is heated. In sections of the target reaching the liquid-vapor regime in a homogeneous state, the system is efficiently cooled along the liquid-vapor coexistence line and no ablation is observed (II); in the non-melted bulk, cooling occurs along the solid-vapor coexistence curve and spallation is suppressed (I). In this context, only those regions expanding above the critical point undergo ablation: here, the split of the dense and macroscopic branches occurs in the supercritical fluid region, thus ruling out the possibility of a phase transition (III and IV). The same behavior has been observed for a 400 ps pulse.[13]

The following results for a 266 nm, 25 ps pulse incident onto a Si(100) substrate confirm a transition to a new ablation regime. Figure. 8 illustrates the thermodynamic pathways obtained at the threshold energy,

$F_{\rm th}^{\rm b} = 0.35$ J/cm^2; the simulation is for a slab originally consisting of 165600 atoms ($10 \times 10 \times 50$ nm^3). Let us first examine a trajectory for a section of the nonablated material (Fig. 8c). Initial heating in the solid occurs essentially at constant volume (F→G). The system eventually crosses the triple line and the superheated material undergoes a first-order phase transition: as it melts, the semiconducting crystal (G) densifies to a metallic liquid (H). The latter is then rapidly heated by an efficient coupling of the laser energy with the "free" electrons via inverse bremsstrahlung (H→I). At the end of the pulse, the system is locally left in a subcritical state at ≈ 7000 K and ≈ 1 GPa. The subsequent scenario is as follows: (i) in order to equilibrate with the ambient gas, the liquid cools by expanding toward the two-phase regime (I→J). (ii) In contrast to near-threshold fs ablation, however, the smaller pressure buildup results in a slower, nonadiabatic, expansion: substantial thermal conduction occurs and the system is efficiently cooled along the binodal (J→K). In other words, no significant superheating of the liquid occurs and, consequently, phase explosion does not take place. The same behavior has been observed across the entire nonablated region (see Figs. 8b and 8d).

In this context, ablation is associated with the regions expanding supercritically, as confirmed by the split of the dense and average branches in Fig. 8a (marked L); this conclusion is supported by a visual inspection of the system which reveals a plume very similar to that of Fig. 2h; the same observations have been made for a 50 ps pulse.[9] Thus, fragmentation is proposed as the dominant matter removal mechanism in metals and semiconductors for $\tau_{\rm L} \gtrsim 10^{-11}$ s;[9] the latter value is probably higher in materials characterized by a larger optical penetration depth.

As a final remark, note that, for the "long" pulses discussed here, ablation is probably better described by a "trivial" fragmentation process: as the pulse duration is continuously increased, the expansion is expected to eventually become slow enough such the equilibrium structure of the fluid is preserved at all times. However, because the latter is not homogeneous at sufficiently low densities, a decomposition into clusters can still take place.

4. SUMMARY AND CONCLUSIONS

We have performed combined molecular-dynamics/Monte Carlo simulations of short-pulse laser ablation of absorbing solids. In particular, we have investigated the thermodynamic evolution of metals and semiconductors irradiated by pulses with durations ranging from 200 fs to 400 ps.

Under femtosecond irradiation, our results confirm the relevance of phase explosion near the threshold energy and reveal a new mechanism at higher energies: fragmentation. In the picosecond regime, the consequences of a relaxation of the system along the liquid-vapor coexistence line on a time scale of a few tens to a few hundreds of ps are twofold: (i) phase explosion is suppressed in this case, thus confirming fragmentation as a dominant mechanism in matter removal with short pulses. (ii) Under irradiation with very long (ns) pulses, this would imply a heating process *along* the binodal, in contrast with the widely-accepted scenario of Miotello and Kelly whereby the system is heated within the liquid-vapor region and undergoes explosive boiling near the spinodal limit.[6] Although a definite picture is not available at present time, our simulations indicate that the conditions assumed in Ref. 6 are not readily met in practice.

ACKNOWLEDGMENTS

This work has been supported by grants from the Natural Sciences and Engineering Research Council of Canada (NSERC) and the *Fonds Québécois de la Recherche sur la Nature et les Technologies* (FQRNT). We are indebted to the *Réseau Québécois de Calcul de Haute Performance* (RQCHP) for generous allocations of computer resources. P. L. also wishes to thank K. Sokolowski-Tinten and L. V. Zhigilei for useful insights.

REFERENCES

1. D. von der Linde and K. Sokolowski-Tinten, "The physical mechanisms of short-pulse laser ablation," *Appl. Surf. Sc.* **154-155**, pp. 1–10, 2000.
2. K. Sokolowski-Tinten, J. Bialkowski, A. Cavalleri, M. Boing, H. Schüler, and D. von der Linde, "Dynamics of femtosecond laser induced ablation from solid surfaces," in *High Power Laser Ablation*, C. R. Phipps, ed., *Proc. SPIE* **3343**, pp. 46–57, 1998.

3. K. Sokolowski-Tinten, J. Bialkowski, A. Cavalleri, D. von der Linde, A. Oparin, J. Meyer-ter-Vehn, and S. I. Anisimov, "Transient states of matter during short pulse laser ablation," *Phys. Rev. Lett.* **81**, pp. 224–227, 1998.
4. L. V. Zhigilei and B. J. Garrison, "Microscopic mechanisms of laser ablation of organic solids in the thermal and stress confinement irradiation regimes," *J. Appl. Phys.* **88**, pp. 1281–1298, 2000.
5. D. Perez and L. J. Lewis, "Molecular-dynamics study of ablation of solids under femtosecond laser pulses," *Phys. Rev. B* **67**, p. 184102, 2003.
6. A. Miotello and R. Kelly, "Critical assessment of thermal models for laser sputtering at high fluences," *Appl. Phys. Lett.* **67**, pp. 3535–3537, 1995.
7. N. M. Bulgakova and A. V. Bulgakov, "Pulsed laser ablation of solids: transition from normal vaporization to phase explosion," *Appl. Phys. A* **73**, pp. 199–208, 2001.
8. D. Perez and L. J. Lewis, "Ablation of solids under femtosecond laser pulses," *Phys. Rev. Lett.* **89**, p. 255504, 2002.
9. P. Lorazo, L. J. Lewis, and M. Meunier, "Short-pulse laser ablation of absorbing solids: from phase explosion to fragmentation," *Phys. Rev. Lett.* **91**, p. 225502, 2003.
10. F. Vidal, T. W. Johnston, S. Laville, O. Barthélemy, M. Chaker, B. Le Drogoff, J. Margot, and M. Sabsabi, "Critical-point phase separation in laser ablation of conductors," *Phys. Rev. Lett.* **86**, pp. 2573–2576, 2001.
11. T. E. Glover, "Hydrodynamics of particle formation following femtosecond laser ablation," *J. Opt. Soc. Am. B* **20**, pp. 125–131, 2003.
12. P. P. Pronko, S. K. Dutta, D. Du, and R. K. Singh, "Thermophysical effects in laser processing of materials with picosecond and femtosecond pulses," *J. Appl. Phys.* **78**, pp. 6233–6240, 1995.
13. D. Perez and L. J. Lewis, "Thermodynamic evolution of materials during laser ablation under pico and femtosecond pulses," *Appl. Phys. A*, in press.
14. D. V. Makhov and L. J. Lewis, "Isotherms for the liquid-gas phase transition in silicon from NPT Monte Carlo simulations," *Phys. Rev. B* **67**, p. 153202, 2003.
15. P. Lorazo, L. J. Lewis, and M. Meunier, in preparation.
16. F. H. Stillinger and T. A. Weber, "Computer simulation of local order in condensed phases of silicon," *Phys. Rev. B* **31**, pp. 5262–5271, 1985.
17. H. Balamane, T. Halicioglu, and W. A. Tiller, "Comparative study of silicon empirical interatomic potentials," *Phys. Rev. B* **46**, pp. 2250–2279, 1992.
18. N. Honda and Y. Nagasaka, "Vapor-liquid equilibria of silicon by the Gibbs ensemble simulation," *Int. J. Thermophys.* **20**, pp. 837–846, 1999.
19. J. Q. Broughton and X. P. Li, "Phase diagram of silicon by molecular dynamics," *Phys. Rev. B* **35**, pp. 9120–9127, 1987.
20. V. K. Shen and P. G. Debenedetti, "A computational study of homogeneous liquid-vapor nucleation in the Lennard-Jones fluid," *J. Chem. Phys.* **111**, pp. 3581–3589, 1999.
21. K. Sokolowski-Tinten, J. Bialkowski, and D. von der Linde, "Ultrafast laser-induced order-disorder transitions in semiconductors," *Phys. Rev. B* **51**, pp. 14186–14198, 1995.
22. Wm. T. Ashurst and Brad Lee Holian, "Droplet formation by rapid expansion of a liquid," *Phys. Rev. E* **59**, pp. 6742–6752, 1999.
23. A. Cavalleri, K. Sokolowski-Tinten, J. Bialkowski, M. Schreiner, and D. von der Linde, "Femtosecond melting and ablation of semiconductors studied with time of flight mass spectroscopy," *J. Appl. Phys.* **85**, pp. 3301–3309, 1999.
24. B. Rethfeld, V. V. Temnov, K. Sokolowski-Tinten, S. I. Anisimov, and D. von der Linde, "Dynamics of ultrashort pulse-laser ablation: Equation-of-state considerations," in *High Power Laser Ablation IV*, C. R. Phipps, ed., *Proc. SPIE* **4760**, pp. 72–80, 2002.